ISBN: 978-3-95450-211-0 doi:10.18429/JACoW-SRF2019-MOP015

RF PERFORMANCE SENSITIVITY TO TUNING OF Nb_3Sn COATED CEBAF CAVITIES

G. Eremeev*, W. Crahen, J. Henry, F. Marhauser, C.E. Reece
Thomas Jefferson National Accelerator Facility, Newport News, VA 23606, U.S.A.
U. Pudasaini
College of William and Mary, Williamsburg, VA 23185, U.S.A.

Abstract

Nb_3Sn has the potential to surpass niobium as the material of choice for SRF applications. The potential of this material stems from a larger superconducting energy gap, which leads to expectations of a higher RF critical field and a lower RF surface resistance. The appeal of better superconducting properties is offset by the relative complexity of producing practical Nb_3Sn structures, and Nb_3Sn sensitivity to lattice disorder challenges the use of the material for practical applications. Such sensitivity is indirectly probed during SRF cavity development, when the cavity is tuned to match the desired accelerator frequency. In the course of recent experiments we have coated and tuned several multicell cavities. Cold RF measurements before and after tuning showed degradation in cavity performance after tuning. The results of RF measurement were compared against strain evolution on Nb_3Sn surface during tuning based on CST and ANSYS models.

INTRODUCTION

Nb_3Sn films deposited into niobium cavities using vapor diffusion technique achieved accelerating gradients E_{acc} close to 20 MV/m and quality factors above $1{\cdot}10^{10}$ at 4.3 K in recent years [1–5]. Given its superheating critical field and superconducting transition temperature, Nb_3Sn superconducting material has the potential to sustain accelerating gradients close to 100 MV/m and quality factors close to $5{\cdot}10^{10}$ at 4.3 K, and R&D efforts are ongoing to understand and improve vapor diffusion deposition technique towards its potential.

In parallel, efforts are ongoing to achieve single-cell cavity performance in practical multicell structures [6]. Over the past couple years a number of CEBAF 5-cell cavities were coated in the JLab coating system towards development of multicell cavity coatings. High quality factors have been measured in Nb_3Sn-coated 5-cell cavities, but the cavities were limited to below E_{acc} = 10 MV/m [6]. Two of the coated cavities were progressed towards assembly into a cavity pair, which could be integrated into a smaller quarter cryomodule. Following the assembly, the cavities were measured as a pair in a vertical dewar and their performance was found to degrade significantly from the qualification tests before the pair assembly [7]. Tuning of the cavities before pair assembly was suspected as one of the potential causes for cavity degradation. Further experiments were conducted to test the tuning sensitivity hypothesis and are described in the subsequent sections.

CAVITY PAIR TESTING

Details of the setup, the coating process, and coating appearance can be found elsewhere [6–8]. In the first attempt to built a two-cavity string, a so-called cavity pair, out of Nb_3Sn coated cavities, a degradation was observed between qualifications tests of individual cavities and the pair test [7]. The cavities used in the experiment were IA110 and IA114 from the original CEBAF production. The qualification test results of these cavities are shown in Fig. 1. The low-field

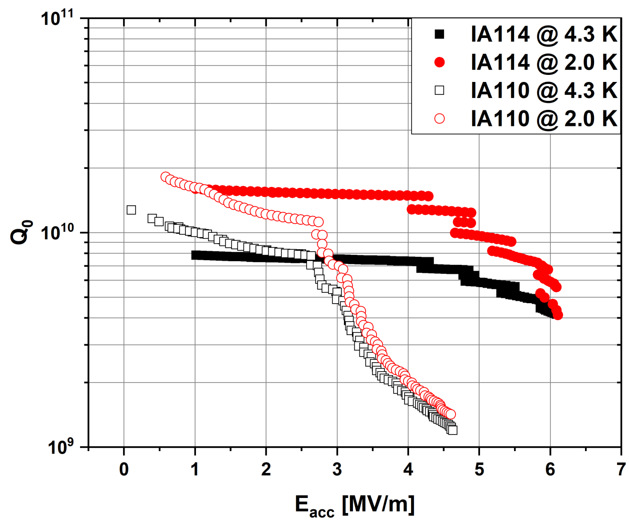

Figure 1: IA114 and IA110 qualification test results at 4 K and 2 K. Discontinuities in Q-curves are due to Q-switches.

Q_0 of IA114 was about $8{\cdot}10^9$ at 4K and $1.5{\cdot}10^{10}$ at 2 K. The quality factor was approximately constant up to about E_{acc} = 4 MV/m. Above E_{acc} = 4 MV/m, several Q-switches were observed at both 4 K and 2 K. The cavity was limited to E_{acc} = 6 MV/m with the quality factor of $4{\cdot}10^9$ at both temperatures. The low-field Q_0 of IA110 was about $1{\cdot}10^{10}$ at 4 K and $1.8{\cdot}10^{10}$ at 2 K. Above E_{acc} = 3 MV/m, several Q-switches were observed at both 4 K and 2 K. The cavity was limited to E_{acc} = 4.5 MV/m with a quality factor of $1.4{\cdot}10^9$ at both temperatures.

After qualification RF tests, both cavities were assembled into a pair and tested. Tested in a pair both cavities exhibited similar quality factors and quality factor field dependence, see Fig. 2. The low-field Q_0 was about $5{\cdot}10^9$ and had a strong field dependence at both 4 K and 2 K. To verify per-

* grigory@jlab.org

ISBN: 978-3-95450-211-0 doi:10.18429/JACoW-SRF2019-MOP015

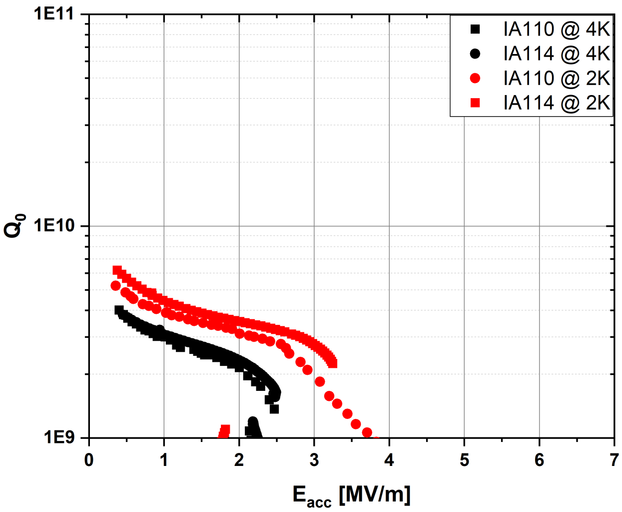

Figure 2: IA110 and IA114 test results after the cavities were assembled into the cavity pair. Note the significant change from qualification tests, Fig. 1.

formance degradation the pair was taken apart, and IA114 was re-HPRed and dried in the cleanroom. IA114 was then assembled to be tested individually with hardware used in the qualification tests after Nb_3Sn coating. The cavity performance was unchanged from the pair test. Lower quality factors and strong Q-slope were observed again, Fig. 3. Tuning before pair assembly was suggested as one of the possible reason for the cavity performance degradation: after qualification tests the π-mode warm resonant frequency of IA110 was tuned from 1493.468 MHz to 1494.650 MHz, and the resonant frequency of IA114 was tuned from 1494.314 MHz to 1494.652 MHz.

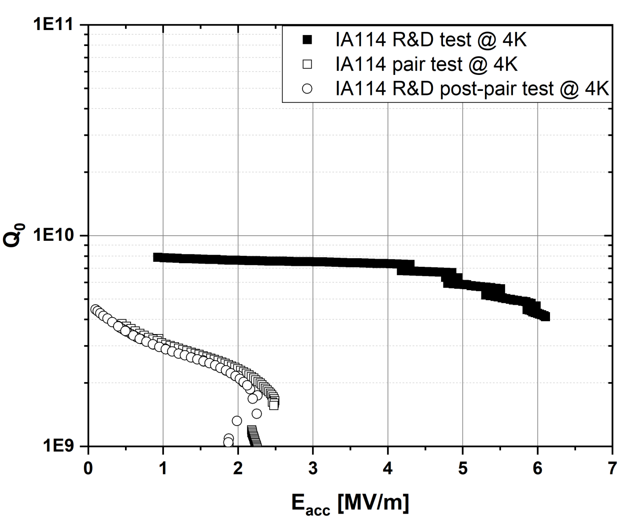

Figure 3: IA114 test results after Nb_3Sn coating (full squares), after pair assembly (open squares), and after reassembly with R&D hardware(open circles).

IMPACT OF CAVITY TUNING

To investigate the tuning sensitivity, IA016 and 5C75-J-002 cavities were coated with Nb_3Sn using our standard process and tested before and after warm tuning of the resonant frequency. IA016 was first tested at 4.3 K after Nb_3Sn coating, Fig. 4. The cavity exhibited a Q_0 of about $6{\cdot}10^9$ at $E_{acc} \approx 1$ MV/m. The quality factor degraded to about $5{\cdot}10^9$ at $E_{acc} = 6$ MV/m. Q-switch was observed at $E_{acc} \approx 6.5$ MV/m, where the quality factor dropped to about $2{\cdot}10^9$. The cavity was limited by a quench at $E_{acc} \approx 8$ MV/m. No further degradation in the quality factor was observed after quenching at the highest field. Following the test the cavity was removed from the dewar, moved to the RF tuning bench, and tuned. The π-mode warm resonant frequency was tuned from 1494.010 MHz to 1493.828 MHz. After tuning the cavity was processed with standard preparation techniques towards RF testing. Cavity test result at 4.3 K is shown in Fig. 4. The cavity exhibited a Q_0 of about $5{\cdot}10^9$ at $E_{acc} \approx 1$ MV/m. The quality factor degraded with field to $2{\cdot}10^9$ at $E_{acc} \approx 3.5$ MV/m, where the cavity was limited by a quench. No degradation in the quality factor was observed after quenching at the highest field. It is noteworthy that the field dependence of the quality factor after tuning is very similar to the field dependence observed in IA110 and IA114 cavity tests after the cavities were assembled into a pair, Fig. 3.

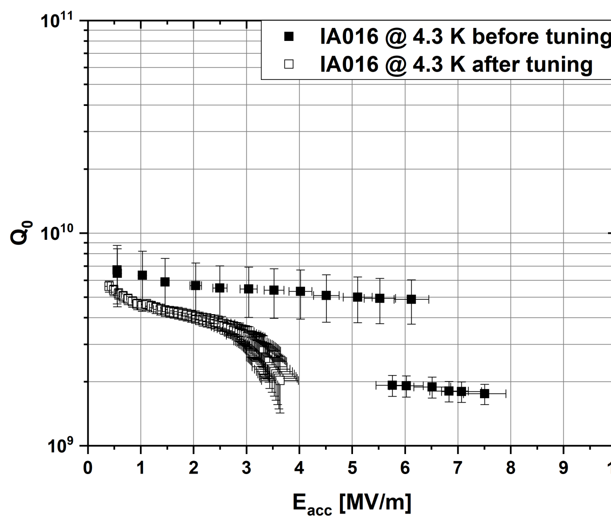

Figure 4: IA016 test result at 4.3 K before and after cavity tuning at room temperature. Note Q-degradation after cavity tuning.

5C75-J-002 was tested at 4.3 K after Nb_3Sn coating before and after cavity tuning at room temperature, Fig. 5. In the first test the cavity had a quality factor of about $8{\cdot}10^9$ at $E_{acc} \approx 1$ MV/m. The quality factor stayed flat up to $E_{acc} \approx 3$ MV/m, where the quality factor degraded with a Q-slope to $2{\cdot}10^9$ at $E_{acc} \approx 6$ MV/m. After the test the cavity was removed from the dewar. Beamline covers were removed and the cavity was placed on the tuning bench. First, the cell #3 was squeezed, which caused a -142 kHz shift in the π-mode

ISBN: 978-3-95450-211-0 doi:10.18429/JACoW-SRF2019-MOP015

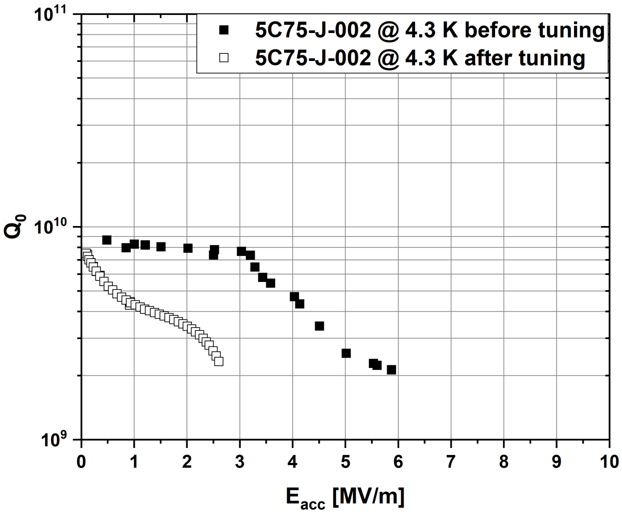

Figure 5: 5C75-J-002 test result at 4.3 K before and after cavity tuning at room temperature. Note Q-degradation after cavity tuning.

frequency from 1494.519 MHz to 1494.377 MHz. Cell #5 was squeezed, which caused a 19 kHz shift in the π-mode frequency from 1494.377 MHz to 1494.396 MHz. Then cell #4 was squeezed, which caused a -64 kHz shift in the π-mode frequency from 1494.396 MHz to 1494.332 MHz. Finally, cell #2 was squeezed, which caused a -86 kHz shift in the π-mode frequency from 1494.332 MHz to 1494.246 MHz. After the last tuning step the cavity was prepared for another RF test following the standard preparation procedures. After tuning the quality factor of the cavity was $4{\cdot}10^9$ at $E_{acc} \approx$ 1 MV/m at 4.3 K. The cavity exhibited a strong Q-slope degrading the quality factor to about $2{\cdot}10^9$ at $E_{acc} \approx 2.6$ MV/m. Again, the field dependence of the tuned cavity is very similar to the field dependence of IA016, IA110, and IA114 after tuning.

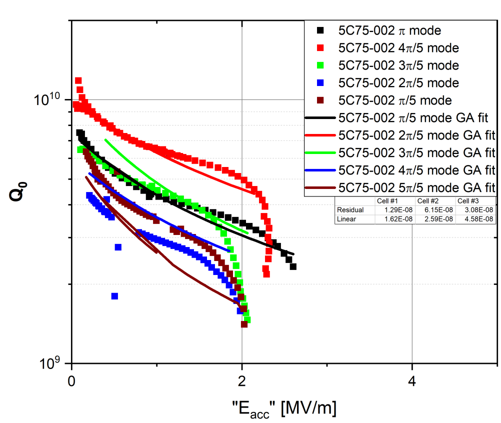

Figure 6: 5C75-J-002 test results for different passband modes at 4.3 K after cavity tuning at room temperature.

To measure how individual cavity cells affect the cavity performance, the quality factor as a function of field was measured after tuning for all the passband modes, Fig. 6. The energy distribution for each passband mode was calculated from the cavity model. The calculation was compared to the passband energy distribution evaluated from beadpull measurements, which were performed after the last tuning step before cold RF test, Fig. 7. For illustration purposes, beadpull data were scaled to overlay the simulated profile. As it can be seen in Fig. 7, the calculated energy distributions have a good agreement with the measurements done on the cavity before the RF test. Each cell was then assumed to have an individual surface resistance and an individual linear field dependence of the surface resistance. Due to the field symmetry of the simulated passband energy distribution, there are only three unique cells. The surface resistance of cell #1 was assumed to be identical to cell #5, and the surface resistance of cell #2 was assumed to be identical to cell #4. The surface resistance and its field dependence was then calculated for each passband mode. The measured passband data and the best fit is shown in Fig. 6. The measured passband data are best fitted assuming 13 nΩ of the surface resistance in end cells, 62 nΩ in the cells #2 and #4, and 31 in the cell #3. The linear field dependence coefficients are $1.6{\cdot}10^{-8}$, $2.6{\cdot}10^{-8}$, and $4.6{\cdot}10^{-8}$, respectively. Simulation of the RF data shows that the best cells were the end cells, which were not tuned. Compared to the end cells, the average of the second and fourth cells showed an increase of 49 nΩ, and the increase in the surface resistance slope by 60 percent. The center cell showed an increase of 18 nΩ and almost a factor of three increase in the slope. The worst performing cells according to the passband measurements were also the cells that were tuned the most during warm tuning.

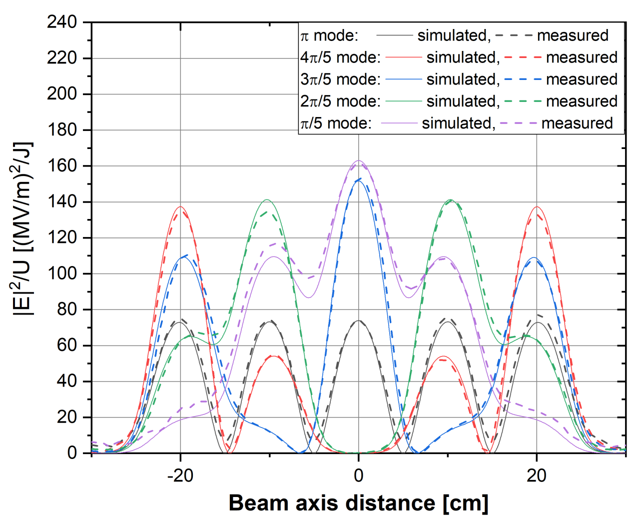

Figure 7: 5C75-J-002 test results for different passband modes at 4.3 K after cavity tuning at room temperature. Passband modes, measured using bead pull technique, were scaled for illustration purposes.

ISBN: 978-3-95450-211-0 doi:10.18429/JACoW-SRF2019-MOP015

TUNING SIMULATIONS

Superconducting properties of Nb_3Sn are known to degrade with strain [9]. One of the possible mechanisms behind the observed degradation in the performance of tuned cavities is the degradation in the superconducting properties due to the induced strain. ANSYS simulation were done to estimate the strain induced during cavity tuning. Due to the spring-back effect the cavity has to be deformed beyond desired tuning point. This effect, which was accounted in simulation, depends strongly on the material parameters. For ANSYS simulations SNS prototype niobium WCL as received was used [10]. RF simulations using CST Microwave

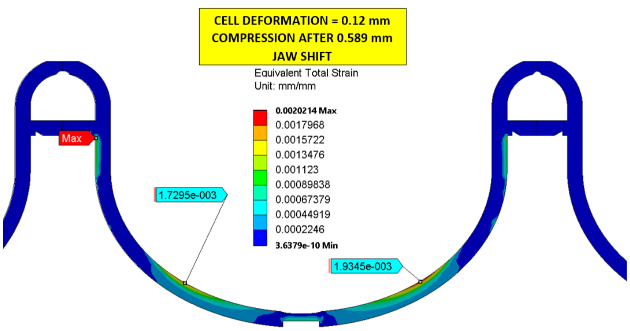

Figure 8: ANSYS tuning simulation of 5C75-J-002 for -0.12 mm wall displacement. Residual cavity shape corresponds to about -150 kHz frequency shift.

Studio showed the frequency shift of -142 kHz corresponds to the wall displacement of about -.12 mm caused by the tuning plates. In Fig. 8, ANSYS simulation corresponding to such wall displacement is shown, which indicates the maximum total strain of about 0.2%. To achieve such frequency shift, the cavity wall was displaced by about -0.589 mm, corresponding to the peak detuning for the simulated material of about -700 kHz. Since this value will depend on material parameters of the specific material, ANSYS simulations were done for -0.5 mm displacement to estimate the peak strain during tuning, Fig. 9. The peak equivalent total strain induced by the tuning in the simulations was located in the equator region and reached 0.45 %.

The expected increase in RF surface resistance can estimated from this calculated induced strain. Under assumption that the strain affects RF surface resistance through degradation in the superconducting transition temperature, the increase in the surface resistance can be estimated using BCS surface resistance approximation:

$$R_{\mathrm{RF}} = \frac{A}{T} e^{-\frac{\Delta}{T}} \quad (1)$$

, where A = 3.89 ± 0.17 Ω/K and Δ = 40.83 ± 0.37 K gave the best fit to the data measured on a Nb_3Sn-coated single cell, ALD3 [2]. Strain of 0.45 % was measured to reduced the superconducting transition temperature by 0.3 K [9]. Assuming that the reduction in the superconducting transition temperature causes the reduction in the gap Δ from 40.83 K

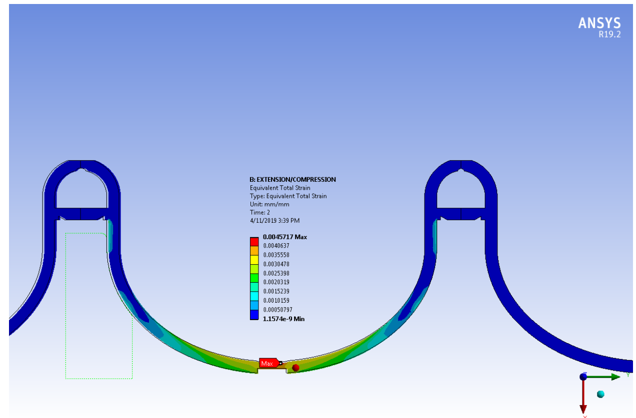

Figure 9: ANSYS tuning simulation of 5C75-J-002 for -0.5 mm wall displacement. Residual cavity shape corresponds to about -600 kHz frequency shift.

to 40.15 K, the RF surface resistance at 4.3 K will increase from 6.7 nΩ to 7.8 nΩ. Hence, the upper bound of the increase in the surface resistance due to induced simulated strain can be estimated at about 1.1 nΩ, which is significantly smaller than more than 18 nΩ increase estimated from RF measurements.

The observed degradation in RF properties of coated Nb_3Sn cavities is not explained by a simple strain-induced gap reduction. One of the possible reasons behind significantly stronger response to tuning could be defects on the surface of coated cavities. ANSYS simulations assumed smooth surface, whereas geometric defects are often observed on the surface of SRF cavities. To simulate the effect

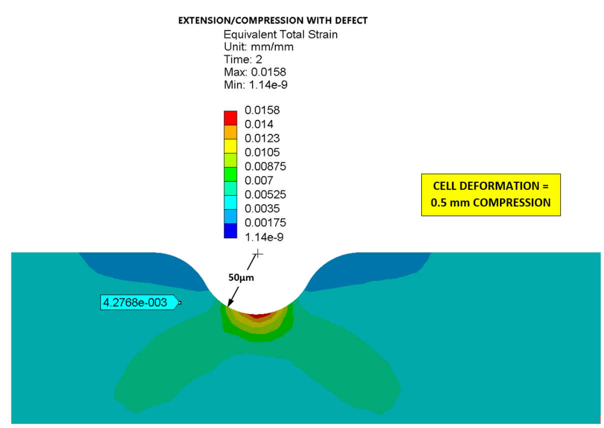

Figure 10: ANSYS tuning simulation of a smooth 50 μm groove located at the equator during -0.5 mm wall displacement. Note the higher strain levels in the pit.

of defects a smooth 50 μm groove in the equator regions was simulated in ANSYS, Fig. 10. The maximum total strain, when such groove was present, was three times higher than what was calculated without a groove, which shows that strain at defects could significantly exceed the strain expected for a defect-free surface, which will lead to stronger

ISBN: 978-3-95450-211-0 doi:10.18429/JACoW-SRF2019-MOP015

degradation and potentially film cracking. The response to tuning for a specific cavity can be expected to depend on the number of defects, their location, and their geometry.

SUMMARY

The appeal of better superconducting properties is offset by the relative complexity of producing practical Nb_3Sn structures, and Nb_3Sn sensitivity to lattice disorder challenges the use of the material for practical applications. Such sensitivity is indirectly probed during SRF cavity development, when the cavity is tuned to match the desired accelerator frequency. In the course of recent experiments we have coated and tuned several multi-cell cavities. Cold RF measurements before and after tuning showed degradation in cavity performance after tuning. Degradation in the transition temperature alone due to the strain induced by tuning cavities to the desired frequencies, which was simulated using CST microwave studio and ANSYS, cannot explain the observed increase in the surface resistance. Strain enhancement and film cracking is suggested as a potential reason behind RF surface resistance increase higher than expected from the simulation.

ACKNOWLEDGMENTS

We thank JLab technical staff for help with some of the cavity preparation and Brian Carpenter, Kirk Davis, John Fischer, Bob Legg, Kurt Macha, Tony Reilly, Bob Rimmer, Scott Williams for useful suggestions.

Co-Authored by Jefferson Science Associates, LLC under U.S. DOE Contract No. DE-AC05-06OR23177. This material is based upon work supported by the U.S. Department of Energy, Office of Science, Office of Nuclear Physics.

REFERENCES

[1] S. Posen and M. Liepe, "RF Test Results of the first Nb3Sn Cavities Coated at Cornell", in *Proc. 16th Int. Conf. RF Superconductivity (SRF'13)*, Paris, France, Sep. 2013, paper TUP087, pp. 666–669.

[2] G. V. Eremeev, M. J. Kelley, C. E. Reece, U. Pudasaini, and J. Tuggle, "Progress With Multi-Cell Nb3Sn Cavity Development Linked With Sample Materials Characterization", in *Proc. 17th Int. Conf. RF Superconductivity (SRF'15)*, Whistler, Canada, Sep. 2015, paper TUBA05, pp. 505–511.

[3] S. Posen, M. Liepe, and D. L. Hall, "Proof-of-principle demonstration of Nb_3Sn superconducting radiofrequency cavities for high Q0 applications", *Appl. Phys. Lett.*, vol. 106, p. 082601, 2015. doi:10.1063/1.4913247

[4] S. Posen and D.L. Hall, "Nb_3Sn superconducting radiofrequency cavities: fabrication, results, properties, and prospects", *Supercond. Sci. Technol.*, vol. 30, p. 033004, 2017. doi:10.1088/1361-6668/30/3/033004

[5] S. Posen, TTC meeting, Vancouver, BC, Canada, 2019. https://indico.desy.de/indico/event/21337/timetable/#20190207.detailed

[6] U. Pudasaini *et al.*, "Nb_33Sn Multicell Cavity Coating at JLab", in *Proc. IPAC'18*, Vancouver, Canada, Apr.-May 2018, pp. 1798–1803. doi:10.18429/JACoW-IPAC2018-WEYGBF3

[7] G. V. Eremeev and U. Pudasaini, "Development of Nb_3Sn Multicell Cavity Coatings", in *Proc. IPAC'19*, Melbourne, Australia, May 2019, pp. 3070-3073. doi:10.18429/JACoW-IPAC2019-WEPRB111

[8] G. V. Eremeev, W. A. Clemens, K. Macha, H. Park, and R. S. Williams, "Commissioning Results of Nb_3Sn Cavity Vapor Diffusion Deposition System at JLab", in *Proc. IPAC'15*, Richmond, VA, USA, May 2015, pp. 3512–3514. doi:10.18429/JACoW-IPAC2015-WEPWI011

[9] M. G. T. Mentink, "An experimental and computational study of strain sensitivity in superconducting Nb_3Sn", Faculty of Science and Technology, University of Twente, Netherlands, Ph.D. dissertation, 2014.

[10] G. Myneni and P. Kneisel, "High RRR Niobium Material Studies", JLab technical note, JLAB-TN-02-01, 2001.